JOURNAL OF AGRICULTURAL AND FOOD CHEMISTRY

Cold-Set Globular Protein Gels: Interactions, Structure and Rheology as a Function of Protein Concentration

ARNO C. ALTING,*,†,‡ ROB J. HAMER,†,§ CEES G. DE KRUIF,†,‡,|| AND RONALD W. VISSCHERS†,‡

Wageningen Centre for Food Sciences, Wageningen, The Netherlands, NIZO food research, Ede, The Netherlands, Wageningen University, Wageningen, The Netherlands, and University of Utrecht, Utrecht, The Netherlands

We identified the contribution of covalent and noncovalent interactions to the scaling behavior of the structural and rheological properties in a cold gelling protein system. The system we studied consisted of two types of whey protein aggregates, equal in size but different in the amount of accessible thiol groups at the surface of the aggregates. Analysis of the structural characteristics of acid-induced gels of both thiol-blocked and unmodified whey protein aggregates yielded a fractal dimension (2.3 ± 0.1), which is in line with other comparable protein networks. However, application of known fractal scaling equations to our rheological data yielded ambiguous results. It is suggested that acid-induced cold-gelation probably starts off as a fractal process, but is rapidly taken over by another mechanism at larger length scales (>100 nm). In addition, indications were found for disulfide cross-link-dependent structural rearrangements at smaller length scales (<100 nm).

KEYWORDS: Cold gelation; disulfide bonds; whey proteins; thiol-blockers; whey protein isolate; fractal theory

INTRODUCTION

Preparation of globular protein gels can be viewed as consisting of three distinct steps: denaturation, aggregation, and gelation. In a typical heat-set or thermotropic gel, these processes are intertwined and occur simultaneously during a one step heating process. In cold-set gels, denaturation and aggregation are separated from the gelation step (*1*). In this procedure, protein aggregates are first prepared by heating a solution of native proteins at a pH well above the isoelectric point of the protein and in the absence of salt. This results in the formation of repulsive aggregates. Second (after cooling), an acid-induced cold-set gel is formed by gradually lowering the pH to the isoelectric point of the protein aggregates (*2*). In this way, aggregation and gelation take place sequentially, which makes it possible to study the direct relationship between aggregate and final gel properties. Also, complications that arise from the use of protein mixtures are less troublesome, because these mainly influence the primary denaturation and aggregation kinetics. Both heat- and cold-set gels of globular proteins are used to improve the texture of dairy products, fresh meat, fresh fish, and surimi. To improve the application of these ingredients, it is important to establish relationships between consumer perception, texture, and mouthfeel on one hand and rheological properties of the protein gels on the other hand. The rheological properties of gels are a complex function of the ingredient composition, microscopic properties, and mesoscopic structures of gel matrixes. Although a direct relationship between rheological parameters and consumer perception seldom exists, it may be feasible to predict how practically relevant food properties scale with the amount of protein.

In the literature, different models exist that describe the scaling behavior of gel properties with the protein concentration. In the so-called cascade model, rheological scaling behavior is related to polymer−polymer interaction and the formation of junction zones (*3*). The concept of fractals (*4*) provides an alternative approach to explaining the scaling behavior of the elastic properties of the aggregate network. In this model, the geometric structure is scale-invariant. A single parameter *D*, called fractal dimensionality, describes the geometric properties of the network for the typical length scales at which the random aggregation mechanism occurs. Several theories have been developed to predict the scaling behavior of micro-structural properties and rheological properties with the protein concentration on the basis of the fractal dimension, in both heat- and cold-set gels (*5*, *6*, *7*, *8*). However, these theories seem not to be applicable in all cases (*9*, *10*). Verheul and Roefs (*11*) clearly demonstrated for heat-set gels of whey protein isolate (WPI) that only a fraction of the protein is aggregated and available for the building of a protein network at the point when the microstructure is formed. In contrast to heat-induced gelation,

* To whom correspondence should be addressed. NIZO food research, P.O. Box 20, 6710 BA, Ede, The Netherlands. Phone: +31 318 659571. Fax: +31 318 650400. E-mail: arno.alting@nizo.nl.
† Wageningen Centre for Food Sciences.
‡ NIZO food research.
§ Wageningen University.
|| University of Utrecht.

10.1021/jf0209342 CCC: $25.00
Published on Web 04/10/2003

with acid-induced cold gelation all the protein is in its aggregated form and available to participate in the protein network from the start of the gelation. Therefore, it may be expected that cold-set gels will better satisfy the conditions for fractal aggregation than heat-set gels do.

The fractal dimension of a particle gel can be derived from different gel properties: the wavelength dependence of the turbidity (*6*, *12*), correlation analysis of confocal scanning laser microscope (CSLM) images (*6*, *13*), and also from the concentration dependence of the permeability coefficient (*6*, *13*, *14*) or the storage modulus (*6*, *13*, *15*). Turbidity, microstructural parameters, and permeability are, in general, not influenced by the interactions between the particles. Rheological properties (storage modulus) on the other hand depend on both the geometry and the connectivity of the protein network.

Here, we aim to identify the contribution of structural and interaction parameters to the rheological properties of cold-set gels of WPI. Previously, we have developed a cold-gelation system, consisting of two types of WPI aggregates, equal in size but different in the amount of accessible thiol groups at the surface of the aggregates (*16*). We demonstrated that the initial microstructure of the gel is mainly determined by noncovalent interactions and is not affected by modifying the amount of disulfide bonds. This is in contrast with the mechanical properties, which can be tuned through changing the amount of reactive thiols present during gelation. Because it is possible with this model system to precisely determine and modify the properties of the WPI aggregates, it should be feasible to identify the individual contributions of covalent and noncovalent interactions to the rheological behavior of protein gels and their scaling with the protein concentration.

In this study, we investigated the scaling behavior of geometrical and rheological properties of acid-induced cold-set WPI-gels. Two different gel systems were characterized: gels made from WPI aggregates with and without thiol-blocking treatment. The results are discussed on the basis of both the gel microstructure and the rheological properties of the gels and are linked to the mechanism of aggregation.

MATERIAL AND METHODS

Reagents and Chemicals. D-gluconic acid lactone (GDL), 5,5′-dithiobis-(2-nitrobenzoic acid) (DTNB), sodium dodecyl sulfate (SDS), and *N*-ethylmaleimide (NEM) were obtained from Sigma Chemicals (St. Louis, Mo. USA). The whey protein isolate (WPI) Bipro was obtained from Davisco Foods International Inc. (La Sueur, MN). The WPI consisted (based on dry weight) of β-Lg (74%), α-lactalbumin (12.5%), bovine serum albumin (5.5%), and immunoglobulins (5.5%). The total amount of proteins in the powder is 97.5%, and it further contains lactose (0.5%) and ash (2%) (*17*).

Preparation of Reactive WPI Aggregates. A 9% solution of WPI aggregates was prepared by heating at 68.5 °C (*16*). The pH after solubilization and heating was 7.2. The solution of WPI aggregates was diluted with filtered (0.22 μm; Millex-GV, Millipore Corporation, Bedford, MA) double-distilled water to different concentrations (0.5−9%) (w/w) and stored at 4 °C. Before storage, the headspace was filled with nitrogen to prevent oxidation of the thiol groups. Sodium azide (0.02% final concentration) was used as a preservative. This heat treatment of a 9% (w/w) WPI solution resulted in a "stable" dispersion of reactive WPI aggregates with a hydrodynamic diameter of 70−80 nm (in a buffer containing SDS), with in excess of 95% of the native proteins participating in aggregate formation (*16*). Under the same conditions, a pure β-lactoglobulin preparation produces aggregates with both comparable size and amount of thiol-exposure (*2*).

Blocking of Free Thiol Groups. Reactive aggregates were treated with NEM at various concentrations (0−5 mM), depending on the protein concentration. The efficiency of the blocking reaction was determined by the use of the Ellman's reagent as previously described (*16*). After addition of the thiol-blocking agents, the reaction was allowed to proceed for at least 30 min at room temperature before further experiments were started. As reported before (*2*, *16*), this modification did not change the size of the WPI aggregates.

Preparation of Acid-Induced Gels. GDL was added as a powder to the WPI solutions to induce cold gelation at ambient temperature. In water, GDL slowly hydrolyses to gluconic acid, causing a gradual reduction in pH toward the isoelectric pH of the protein aggregates. The total amount of GDL required depends on the protein concentration (*18*). Different amounts had to be added to reach a pH of around 5 after approximately 24 h of incubation at ambient temperature. Amounts of 0.06%, 0.10%, 0.12%, 0.14%, 0.23%, 0.42%, and 0.63% (w/w) were added to 0.5, 1, 1.5, 2, 3, 6, and 9% protein-solutions, respectively, to reach a pH value of around 5. The acidification induced gelation of the dispersion of WPI aggregates.

Solubilization of Gels. To determine the size of the aggregates after gelation, gels were solubilized with 3 parts of 20 mM Bis-Tris buffer (pH 7.0) 5% SDS and were held at ambient temperature while constantly stirred. After overnight incubation, no gel particles could be observed with a standard microscope (at 400 × magnification).

Dynamic Light-Scattering Experiments. Dynamic light-scattering (DLS) experiments were performed as outlined by Verheul et al. (*19*). Before analysis, samples were filtered through a low-protein-binding membrane (5 μm; Millex-SV, Millipore Corporation).

Turbidity Measurements. Turbidity measurements were performed at 25 °C on a Cary 1E UV−Vis spectrophotometer (Varian Nederland BV, The Netherlands) equipped with a temperature controller. The turbidity was measured with time as the absorbance at 500 nm, with the pH being monitored simultaneously. Samples were measured in quartz cuvettes with a path length of 2 mm.

Permeability Measurements. Permeability measurements were performed as extensively described by Verheul and Roefs (*11*) and based on a method of Van Dijk and Walstra (*20*). Briefly, a 9% (w/w) solution of WPI aggregates was diluted to different concentrations (0.5−9%) with double-distilled water. Gels were prepared at ambient temperature in open glass tubes (25 cm × 3.7 mm). Approximately 24 h after the addition of GDL, they were placed in a measuring device to monitor the flow of solvent (double-distilled water, pH 5) under hydrostatic pressure. Mean permeability coefficients were determined by measuring the flux of solvent with time of 12 different tubes, using Darcy's law. Within experimental accuracy, the permeability coefficient of WPI gels did not change with time during the experiment.

Assuming that the structure of the network of the cold-set WPI gels can be considered as fractal, the permeability (B) and the volume fraction (φ) or the concentration of the WPI aggregates are related through the following equation derived by Bremer (*6*):

$$B = (a^2/K)\varphi^{2/(D_f-3)} \quad (1)$$

where K is a constant, D_f is the fractal dimension, and a is the radius of the primary particles.

CSLM. Imaging was performed using a Leica confocal scanning laser microscope, type TCS−SP, configured with an inverted microscope and an ArKr laser for single-photon excitation. The protein gels were stained by applying 2 μL of an aqueous solution of 0.05% (w/v) Rhodamine B. The 568 nm laser line was used for excitation, inducing a fluorescent emission of Rhodamine B, detected between 600 and 700 nm.

The fractal dimension of the CSLM images was obtained using a box-counting algorithm, which has the advantage that it does not assume a linear relation between the intensity of the CSLM micrographs and the local protein concentrations. Digitized CSLM images were first thresholded at the mean intensity and 20% above and below this value to determine the boundary between protein and solvent. Then, a closing operation (dilution followed by erosion) was performed to fill the gaps between closely spaced pixels in the image. This operation was followed by an opening operation (erosion followed by dilation) to remove small dark regions in the background of the images (*21*). Subsequently, a square mesh of a certain size L was laid over the outline of the objects on the digitized images. The number of mesh boxes, $N(L)$, that contain

Table 1. Exponent *A* and *B* in the Equations $G' \propto \varphi^A$ and $\gamma_0 \propto \varphi^B$, According to Bremer, 1992 and Shih et al. (1990)[a]

A	B	reference
$2/(3-D_f)$	0	(straight strands) Bremer, 1992
$3/(3-D_f)$	$1/(D_f-3)$	(curved strands) Bremer, 1992
$(3+x)/3-D_f)$	$-(1+x)/(3-D_f)$	(strong-link regime) Shih et al., 1990
$1/(3-D_f)$	$1/(D_f-3)$	(weak-link regime) Shih et al., 1990

[a] The relationships between G′, γ_0, and φ given by Mellema (2000) and Wu and Morbidelli, (2001) are extensions of the models given.

part of the outline of the objects was counted. The fractal dimension, *D*, of the protein aggregates in a two-dimensional projection was calculated from the slope of the double logarithmic plot for $N(L)$ against L, considering the relationship between the parameters

$$N(L) \sim L^{-D} \tag{2}$$

Determination of *D* on the basis of the contour lines of the geometric structures circumvents the problem that the relation between observed fluorescence intensity and actual protein concentration is probably not linear. All operations were performed with the public domain program ImageJ (developed at the U.S. National Institutes of Health and available on the Internet at http://rsb.info.nih.gov/ij/). The fractal dimension of protein aggregates in three dimensions D_f, can be calculated from the following equation (*6*):

$$D_f = D + 1 \tag{3}$$

Rheological Measurements. Small-amplitude oscillatory measurements were made with a Carri-Med CLS^2 500 rheometer (TA Instruments, Leatherhead, UK) using a conical concentric cylinder measuring unit (inner radius 8.60 mm, outer radius 9.33 mm). Immediately after the addition of GDL, samples were brought into the measuring unit and covered with a thin layer of paraffin oil to prevent evaporation. All experiments were conducted in oscillation at a frequency of 1 rad/s (0.159 Hz). First a strain sweep, G(γ), was recorded, and the part of the strain sweep where the storage modulus was independent of strain was taken as the linear region. The formation of a gel network for both the blocked and unmodified aggregates at different protein concentrations was followed by the development of G′ and G″ with time. Gelation and aging of the gels were monitored at 25 °C. Because the network formation during gelation will probably be more sensitive to deformation, a strain at the beginning of the linear region was chosen (1%). The frequency sweeps were performed within the linear region. In these experiments, the frequency was varied from 0.01 to 20 Hz at a temperature of 25 °C.

In an ideal network model, all particles are arranged in a statistical network of chains that all contribute to the same extent to the rigidity of the network. Because it is not generally found that the rigidity of a gel is proportional to the particle concentration, aggregate network models have been developed, and the concept of fractal geometry was introduced. In these models, a particle gel is made up of fractal flocs. The flocs themselves are made up of strands of primary particles (*6*). Different aggregate network models are proposed in the literature to translate rheological data into information about the interactions between aggregating particles, the fractal dimension, and the aggregation mechanism (*5*, *6*, *7*, *8*). In general

$$G' \propto \varphi^A \tag{4}$$

$$\gamma_0 \propto \varphi^B \tag{5}$$

The storage modulus (G') and the limit of linearity (γ_0) will strongly depend on the way the clusters are linked to each other. The exponent *A* in equation 4 and *B* in equation 5 will therefore vary with the particle gel system studied (**Table 1**).

RESULTS AND DISCUSSION

Microstructural Measurements. CSLM and permeability measurements were made at protein concentrations (WPI aggregates) ranging from 0.5 to 9%. Gelation, under the conditions applied, occurred at a minimal protein concentration of 0.5% (9% diluted to 0.5%) for unmodified aggregates. Gels made from thiol-blocked aggregates were much weaker. A protein concentration of 1.5−2% was needed to form a gel that could withstand gravity and handling. In all cases, turbid gels were formed. Gels made from blocked aggregates showed some syneresis and some spontaneous gel fracture after 16 h that increased with time.

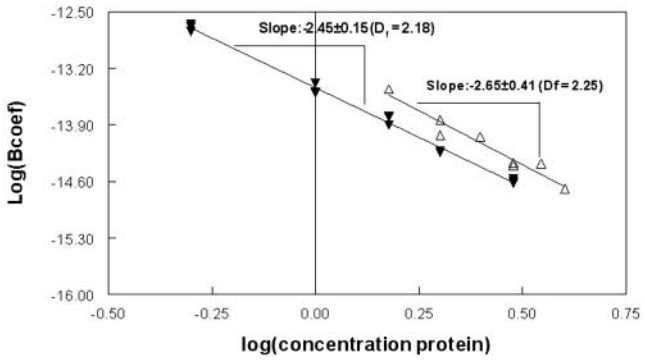

Figure 1. Double logarithmic plot of the protein concentration dependence on the permeability coefficient (m^2) of acid induced gels of blocked (open symbols) and unmodified WPI aggregates (concentration in percent weight/weight) (closed symbols).

Figure 1 shows that the permeability of the gels (B_{gel}) decreased with increasing concentration of WPI aggregates. This indicates that the pores in the gel are smaller when more protein is present. The permeability of the different acid-induced cold-set WPI-gels (B_{gel}) did not change between 24 and 72 h after addition of GDL. At protein concentrations higher than 4%, the flow of liquid through the gel matrix was too low to perform reliable permeability measurements. A linear relationship was observed between B_{gel} and the WPI concentration in a double logarithmic plot (**Figure 1**). B_{gel} decreases by almost 2 orders of magnitude between a protein concentration of 0.5 and 3%. The lines drawn are fitted lines, the slope of which corresponds to a power law with an exponent of around −2.5 and is not significantly different for gels of both the unmodified and blocked aggregates (95% confidence limit).

The results indicate that, within the error of this experiment, the scaling behavior is the same for both types of gels. It must be noted that measurements at other protein concentrations revealed a small difference in permeability between gels made from solutions of blocked aggregates and those made from unmodified aggregates. This is in contrast to an earlier observation (*16*), where the permeability was determined at a single protein concentration of 2% and was not significantly different. The difference in pore size can probably be explained by a difference in the rate of structural rearrangements during aggregation and gelation. To further investigate this, acid-induced gelation was followed by measurement of the turbidity with time (**Figure 2**). The initial rapid onset of the turbidity took place at the same pH (*16*) and reflected the formation of a protein network. Once the network was formed, differences were observed for the two types of aggregates in the steady increase of the turbidity with time, suggesting different kinetics of structural rearrangements.

As a consequence of the acidification, electrostatic repulsion decreases and tenuous clusters of aggregates are formed by physical interactions (*2*). Such open clusters of aggregates are thermodynamically unstable in comparison with a denser cluster, in which more physical bonds can be formed (*6*). In the case of

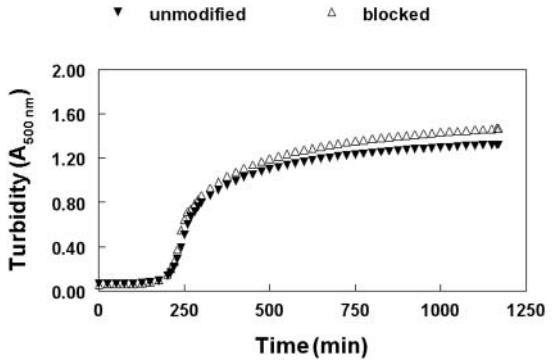

Figure 2. Development of the turbidity of solutions of blocked (open symbols) and unmodified aggregates (closed symbols) (protein concentration 2%) during acid-induced gelation.

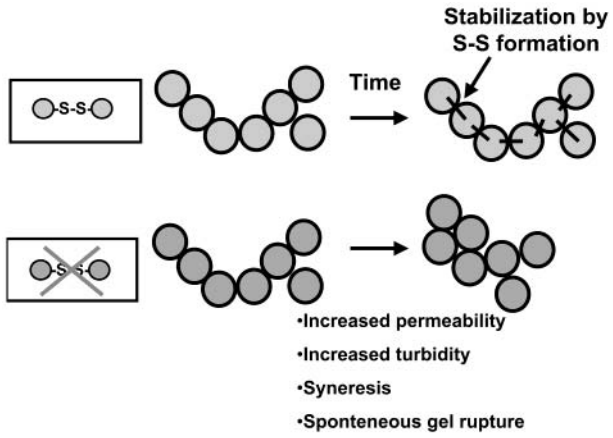

Figure 3. Schematic representation of the occurrence of structural rearrangements.

unmodified aggregates, the initial tenuous structure of these clusters can be (partly) stabilized by the formation of additional covalent disulfide bonds. Blocked aggregates are not able to form these additional stabilizing bonds. As a result of the intrinsic instability, rearrangements can occur much faster, which leads to locally denser clusters and larger pores. This will result in a more turbid gel and a more permeable microstructure (**Figure 3**), which is in line with our observations. As far as we know, no other observations have been reported of a direct relationship between disulfide bond formation and structural rearrangements. As we observed, the rearrangements also cause more syneresis.

The permeability results were also compared with the work of Verheul and Roefs (*11*, *14*). In their studies, heat-induced gels were prepared from WPI at the same heating temperature as applied in our first step of the cold-gelation process, but at other pH values and at higher concentration of salt. By application of the cold-gelation method, gels can be prepared with the same permeability characteristics but at a much lower protein concentration than with heat-induced gelation (0.5 and 3%, respectively).

CSLM images were made from gels prepared with the two types of WPI aggregates for five different protein concentrations (Results not shown). The protein network structure of both types of gels appeared coarser, having larger pores at lower protein concentrations. At a protein concentration of 1%, a thin network of threaded protein material is observed that encloses large holes (3 μm) filled with solvent. Increasing the protein concentration results in smaller, but to the eye similar, structures. At the highest concentrations (>6%) the structures become too small

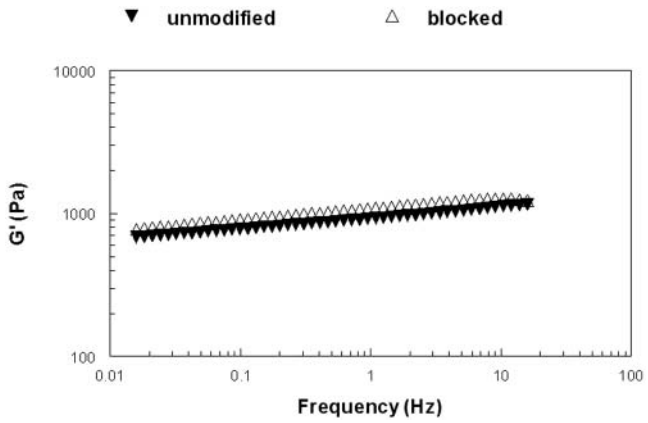

Figure 4. Frequency dependence of the storage modulus (G') of acid-induced WPI gels at a protein concentration of 2% (frequency sweep). Blocked aggregates (open symbols) and unmodified WPI aggregates (closed symbols).

to be fully resolved by the microscope (<0.5 μm). Thus, a more compact network, with smaller pores, was formed when the concentration of protein was increased. There appeared to be no significant differences between the images of the gels prepared from blocked or unmodified aggregates at a protein concentration ranging from 1 to 9%. This is in agreement with our previous observation that blocking the thiol groups on the WPI aggregates did not result in a different microstructure (μm length scale) of the cold-set gel at a protein concentration of 2%, as determined by CSLM (*16*) and small angle light scattering (De Hoog and Alting, unpublished results). Therefore, we conclude that the differences in structural rearrangements occur on a length scale below the resolution of this technique (<200 nm).

Small and Large Deformation Measurements. In contrast to the geometrical gel properties discussed above, larger differences between the two types of aggregates may be expected in rheological measurements, as the rheological properties of the gels studied will depend on both the microstructure of the gel and the interactions between the aggregating particles. The mechanical properties of a gel were monitored during gelation using nondestructive, dynamic measurements. Only the results of G' are presented, because G' and G'' developed simultaneously with time, and the elastic component was more dominant than the viscous component. The elastic behavior of the gels also finds expression in the frequency dependence of the storage modulus (**Figure 4**). Forty hours after the addition of GDL, the frequency dependence of G' was determined for both types of aggregates at a protein concentration of 2%. The dependence of G' on the frequency was the same for both type of aggregates. The storage modulus of purely elastic materials is frequency independent. However, food gels usually have a small contribution of the viscous component, G'', resulting in frequency-dependent G' values reflecting relaxation of these viscous components (*22*). Acid-induced cold-set gels also show this viscoelastic behavior, with G' increasing slightly with increasing frequency.

Figure 5 shows that the initial increase in the storage modulus for gels prepared from unmodified and blocked aggregates did not differ. This is in agreement with our previous observation that the initial kinetics of gelation were not disturbed by blocking the thiol groups (*16*, *23*). Over time, the storage moduli of the gels from the blocked aggregates (only physical interactions) reach a plateau value, whereas for the moduli of gels prepared from the unmodified aggregates, it takes a much longer time

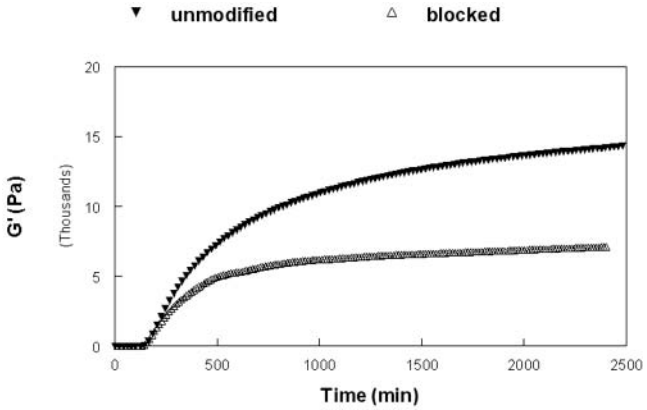

Figure 5. Development of the storage modulus (G') for a 6% (w/w) solution of WPI aggregates (time sweep) (closed symbols unmodified aggregates, open symbols blocked aggregates).

Table 2. Time Dependence of Formation of Disulfide-Linked Aggregates during Acid-Induced Cold Gelation of a 2% (w/w) Solution of WPI Aggregates

	Gel prepared from unmodified aggregates[a]		Gel prepared from blocked aggregates[a]	
time[b] (h)	diameter (nm)[c]	intensity (cps × 1000)[c]	diameter (nm)[c]	intensity (cps × 1000)[c]
0	83 ± 1	78	82 ± 1	96
16	167 ± 3	193	83 ± 1	96
24	451 ± 6	471	85 ± 1	95
40	465 ± 11	485	86 ± 1	101
48	512 ± 10	530	84 ± 1	97

[a] Gels were dissolved in SDS-buffer system (1:3)(final protein concentration 0.5%). [b] Time after addition of GDL. [c] Determined by DLS (see Material & Methods section). Errors represent the standard error of the cumulant fits within one measurement.

until a plateau value is reached. In this case, as well as physical interactions, formation of additional disulfide bonds is to be expected. **Table 2** clearly shows that with time, disulfide-linked aggregation led to an increase in aggregate size observed after solubilization of the gels (2% (w/w) protein). Pretreatment of the aggregates with a thiol-blocking agent prevented the formation of larger disulfide-linked aggregates. After addition of GDL, no increase in the apparent diameter of thiol-blocked aggregates with time as determined by DLS was observed.

To predict the plateau G'(inf) values at infinite times, we fitted both first-order reaction kinetics and (irreversible) second-order kinetics (*24*) to the cure curves. We found negligible differences in the obtained G'(inf) between the two types of fits, so we cannot draw conclusions about the actual kinetic mechanism of gelation from these cure curves. However, because both types of fits display significant differences between the unmodified and blocked aggregates, we further analyzed the G'(inf) values as a function of protein concentration for these two systems. From **Figure 6**, it can be seen that the storage modulus (plateau-value) of the gels increased with increasing protein concentration (from 1 to 9% (w/w) protein). The values of (d log G')/(d log C) of gels prepared from blocked aggregates (only physical interactions) or prepared from unmodified aggregates (both physical and covalent interactions) were significantly different irrespective to the type of fit applied. In the absence of thiol groups on the WPI aggregates, this led to a (d log G')/(d log C) of 2.05 ± 0.18. (95% confidence limit). The lines drawn are linear fits to the experimental points, and the line is steeper for

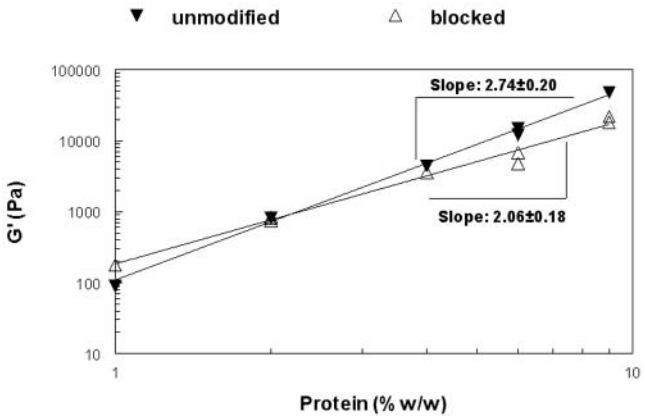

Figure 6. Protein concentration dependence of the storage modulus (G') of acid-induced WPI gels (closed symbols unmodified aggregates, open symbols blocked aggregates).

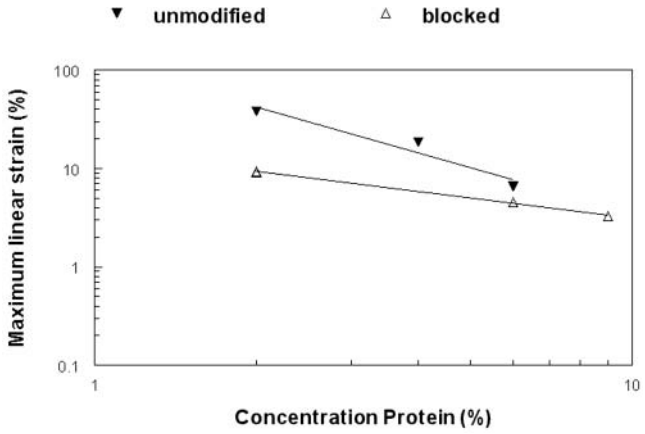

Figure 7. Maximum linear strain of acid-induced WPI gels at different protein concentrations (strain sweep), determined 40 h after the addition of GDL (closed symbols unmodified aggregates, open symbols blocked aggregates).

the unmodified WPI aggregates, with a slope of 2.75 ± 0.20 (95% confidence limit).

Surprisingly, at protein concentrations lower than 2% (w/w) the G' plateau values were higher for cold-set gels prepared from blocked aggregates. As for the microstructural observations, this can be explained by the occurrence of structural rearrangements during the initial stage of the gelation process, resulting in denser packing and more physical interactions and, therefore, higher G' values. At higher protein concentration, this process is frustrated and dominated by the formation of disulfide bonds (**Figure 3**).

Forty hours after the addition of GDL, the maximum linear strain was determined for both types of aggregates (2−9% protein). The maximum linear strain decreased only slightly with increasing protein concentration (**Figure 7**). The maximum linear strain of the unmodified aggregates appears to be more dependent on the protein concentration, and the values of the unmodified aggregates at the different protein concentrations were higher than the values of the blocked aggregates. Strain sweep experiments performed on gels that were cured for 24 h confirmed these trends (data not shown).

The rheological results support the idea that the first stage of the cold-gelation process is driven by physical interactions (*2*, *16*). Gelation of the blocked aggregates can be considered as a one-stage process. Only physical interactions were involved in the gelation process leading to the formation of a space-filling

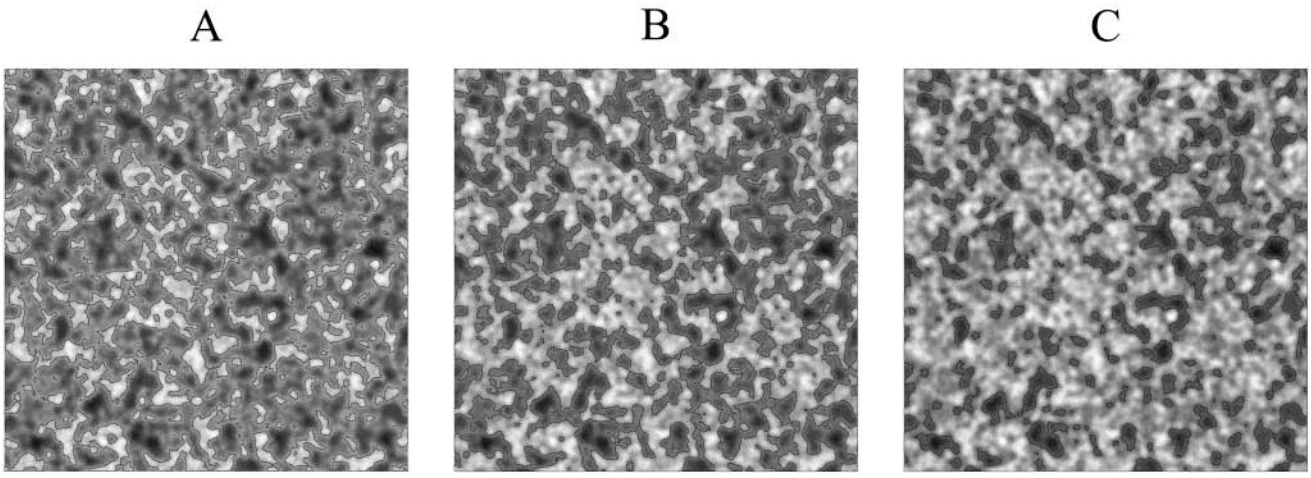

Figure 8. Digitization of a CSLM image of a 2% WPI-gel (unmodified aggregates) at three different threshold values, 30% (A), 50% (B) and 70% (C). The images represent a total surface of 20 × 20 μm.

gel network. No increase in disulfide-linked aggregation with time was observed. In contrast, the gelation process of unmodified aggregates can be considered as a two-stage process. The first stage represents the formation of the gel by physical aggregation, the second stage represents an increase in the gel stiffness and hardness by formation of additional covalent bonds between the structural elements of the gel. This is reflected by a time-dependent increase in G' and hardness and by the formation of larger disulfide-linked aggregates. The difference in the type of gelation process, one- or two-stage, leads to different mechanical properties at the same protein concentration. At lower protein concentrations (<2% (w/w)), the stabilizing role of the disulfide bonds formed is less pronounced, allowing the occurrence of structural rearrangements.

Fractal Nature. If it is assumed that the aggregation process leading to a space-filling network proceeds as a fractal aggregation process, the difference in slope of the double logarithmic plots of both structural and rheological measurements should give insight into the different interactions between the aggregating particles, relating macroscopic to microscopic properties. From the slope of the permeability versus the protein concentration in a double logarithmic plot, a fractal dimension of 2.2 (± 0.1) was found for the acid-induced cold-set gels. The fractal dimension calculated suggested a reaction-limited aggregation mechanism (*25*). A value between 1.8 and 2.0 would have suggested a diffusion-limited type of aggregation mechanism. These results were in good agreement with the results from the box-counting algorithm applied to the digitized CSLM-images (contour representation) (**Figure 8**) (fractal dimension of 2.3 ± 0.1) and with data from other types of cold-set gels reported in the literature (see below). An important observation was that the different imposed thresholds for determining contours did not greatly influence the value of the fractal dimension.

Fractal geometry has been previously used to characterize structures of salt- or acid-induced protein gels (*6*, *13*, *26*). For GDL-acidified and microbial-acidified milk, a fractal dimension ranging from 2.3 to 2.4 was found by quantitative analysis of CSLM images and by permeability analysis performed at different protein concentrations (*6*, *13*). For salt-induced cold-set gels of WPI, a fractal dimension ranging from 2.3 to 2.6 was found depending on the concentration of salt added (*26*).

Thus, scaling behavior of microstructural parameters yielded power law relations and D_f values that were comparable to ones reported in the literature for other cold-set protein gels. However, our rheological data did not fit within one of the reported fractal aggregate network models (*5*, *6*, *7*, *8*). This is in line with De Kruif et al. (*9*), who observed that application of the scaling laws of Bremer and Shih et al. to heat-induced WPI gels did not result in consistent or realistic values. None of the models mentioned yields realistic scaling parameters when trying to combine the concentration dependence of both small (storage modulus (**Figure 6**)) and large deformation measurements(limit of linearity (**Figure 7**)). Also, Ikeda et al. (*10*) observed that for heat-induced WPI gels under certain conditions, the dependence of the limit of on the protein concentration is incorrectly predicted by fractal models.

A likely explanation for the fact that none of the known models consistently described our data could be that acid-induced aggregation indeed starts off as a random fractal aggregation, but at a certain length scale was frustrated or taken over by another mechanism. Recently, it has been proposed for heat- and solvent quality(ethanol)-induced globular protein gelation that, during gelation, both demixing by gelation and binary phase separation occurred (*27*, *28*, *29*). Indeed, in preliminary aggregation experiments with our system, where the aggregation of blocked and unmodified aggregates (protein concentration 0.5%) was monitored by small-angle light scattering, spinodal decomposition was observed (R. H. Tromp, personal communication). If indeed spinodal decomposition occurs, this will lead to locally higher concentrations of (unmodified) aggregates, allowing the formation of disulfide bonds in those concentrated areas, yielding an increase in aggregate size after gelation and resolubilization. The formation of larger disulfide-linked aggregates has indeed been demonstrated (*16*). This implies that the resulting spatial distribution of the disulfide links was not of a purely fractal nature. Although the microstructures of gels made from blocked or unmodified aggregates did not differ (length scale > 100 nm), the difference in the spatial distribution of larger disulfide-linked aggregates will certainly have affected the rheological properties and the applicability of the different fractal models.

Moreover, it was also observed that once a gel was formed, structural rearrangements probably occurred during aging of the gels. The occurrence of rearrangements was more pronounced for the blocked aggregates. These changes in microstructure can take place at a length scale smaller than 100 nm and could affect gel parameters such as the storage modulus and limit of linearity and therefore the applicability of the fractal models. It should be mentioned that this study was limited to the final gelation process and consequently covers only a limited protein con-

centration range. At lower concentration, the spinodal decomposition may be less pronounced, and during the initial heating step when no gel is formed, the rearrangements as discussed here will not occur. This may explain why, under these conditions, fractal scaling over many orders of magnitude of light-scattering intensities can be measured (*30*, *31*).

In conclusion, the rheological data support our hypothesis that the first stage of the cold-gelation process leading to a space-filling protein network is driven by physical interactions (*2*, *16*). The second stage is characterized by an increase in the gel stiffness and hardness by formation of additional covalent bonds between the structural elements of the gel. Analysis of the structural characteristics of acid-induced gels of both thiol-blocked and unmodified WPI aggregates yielded a fractal dimension (2.3 ± 0.1), which is in line with other comparable protein networks and suggests a reaction-limited aggregation mechanism (*25*). However, application of known fractal scaling equations to our rheological data yielded ambiguous results. Probably, gelation starts off as a fractal process but is frustrated by another mechanism at larger length scales (>100 nm). In addition, evidence was found for structural rearrangements at smaller length scales (<100 nm). These rearrangements were enhanced by the loss of the ability to form disulfide cross-links and will also disrupt the applicability of the concept of fractals on acid-induced cold-set gels of whey proteins.

ACKNOWLEDGMENT

The authors thank Panagiota Vrioni and Maria Berki for their help in carrying out the permeability measurements, Jan van Riel for performing the CSLM measurements, Saskia de Jong for helpful advice concerning the rheological measurements, Charles Slangen for carrying out the statistical analysis, and Ton van Vliet for helpful discussions and critical reading of the manuscript.

LITERATURE CITED

(1) Bryant, C. M.; McClements, D. J. Molecular basis of protein functionality with special consideration of cold-set gels derived from heat-denatured whey. *Trends Food Sci. Technol.* **1998**, *9*, 143−151.

(2) Alting, A. C.; de Jongh, H. J. J.; Visschers, R. W.; Simons, J. F. A. Physical and chemical interactions in cold gelation of food proteins. *J. Agric. Food Chem.* **2002**, *50*, 4674−4681.

(3) Ross-Murphy, S. B. Physical gelation of synthetic and biological macromolecules. In *Polymer gels, fundamentals and biomedical applications*, DeRossi, D., Kajiwara, K., Osada, Y., Yamauchi, A. Eds. Plenum Press: New York and London, 1991.

(4) Mandelbrot, B. B. *The fractal Geometry of Nature*; Freeman: New York, 1983.

(5) Shih, W.-H.; Shih, W. Y.; Kim, S.-I.; Liu, J.; Aksay, I. A. Scaling behavior of the elastic properties of colloidal gels. *Preview A.* **1990**, *42*, 4772−4779.

(6) Bremer, L. Fractal aggregation in relation to formation and properties of particle gels. Ph.D. Thesis, Wageningen Agricultural University, 1992.

(7) Mellema, M. Scaling relations between structure and rheology of aging casein particle gels, Ph.D. Thesis, University and Research centre Wageningen, 2001.

(8) Wu, H.; Morbidelli, M. A model relating structure of colloidal gels to their elastic properties. *Langmuir* **2001**, *17*, 1030−1036.

(9) De Kruif, C. G.; Hoffmann, M. A. M.; van Marle, M. E.; van Mil, P. J. J. M.; Roefs, S. P. F. M.; Verheul, M.; Zoon, N. Gelation of proteins from milk. *Faraday Discuss*. **1995**, *101*, 185−200.

(10) Ikeda, S.; Foegeding E. A.; Hagiwara, T. Rheological study on the fractal nature of the protein gel structure. *Langmuir* **1999**, *15*, 8584−8589.

(11) Verheul, M.; Roefs, S. P. F. M. Structure of whey protein gels, studied by permeability, scanning electron microscopy and rheology. *Food Hydrocolloids* **1998**, *12*, 17−24.

(12) Horne, S. Determination of the fractal dimension using turbidimetric techniques. *Faraday Discuss. Chem. Soc.* **1987**, *83*, 259−270.

(13) Van Marle, M. E. Structure and theological properties of yoghurt gels and stirred yoghurts. Ph.D. Thesis, University Twente, 1998.

(14) Verheul, M.; Roefs, S. P. F. M. Structure of particulate whey protein gels: the effect of NaCl concentration, pH heating temperature, and protein composition. *J. Agric. Food Chem.* **1998**, *46*, 4909−4916.

(15) Van Vliet, T.; Keetels, C. J. A. M. Effect of preheating of milk on the structure of acidified milk gels. *Neth. Milk Dairy J.* **1995**, *49*, 27−35.

(16) Alting, A. C.; Hamer, R. J.; de Kruif, C. G.; Visschers, R. W. Formation of disulfide bonds in acid-induced gels of preheated whey protein isolate. *J. Agric. Food Chem.* **2000**, *48*, 5001−5007.

(17) Tuinier, R.; Dhont, J. K. G.; De Kruif, C. G. Depletion-induced phase separation of aggregated whey protein colloids by an exocellular polysaccharide. *Langmuir* **2000**, *16*, 1497−1507.

(18) De Kruif, C. G. Skim milk acidification. *J. Colloid Interface Sci.* **1997**, *185*, 19−25.

(19) Verheul, M.; Roefs, S. P. F. M.; de Kruif, C. G. Kinetics of heat-induced aggregation of β-lactoglobulin. *J. Agric. Food Chem.* **1998**, *46*, 896−903.

(20) Van Dijk, H. J. M.; Walstra, P. Syneresis of curd. 2. One-dimensional syneresis of rennet curd in constant conditions. *Neth. Milk Dairy J.* **1986**, *40*, 3−30.

(21) Russ, J. C. *The image processing handbook*, 3rd ed.; CRC press LLC: Boca Raton, FL, and Springer-Verlag GmbH & Co. KG: Heidelberg, Germany, 1998.

(22) Clark, A. H.; Ross-Murphy, S. B. Structural and mechanical properties of biopolymer gels. In *Advances in Polymer Science*. Springer: Berlin, Germany **1987**, *83*, 57−192.

(23) Vasbinder, A.; Alting, A. C.; Visschers, R. W.; De Kruif, C. G. Texture of acid milk gels: formation of disulfide cross-links during acidification. *Int. Dairy J.*, in press.

(24) Clark, A. H.; Kavanagh, G. M.; Ross-Murphy, S. B. Globular protein gelation-theory and experiment. *Food Hydrocolloids* **2001**, *15*, 383−400.

(25) Vreeker, R.; Hoekstra, L. L.; den Boer, D. C.; Agterof, W. G. M. Fractal aggregation of whey proteins. *Food Hydrocolloids* **1992**, *5*, 423−435.

(26) Marangoni, A. G.; Barbut, S.; McGauley, S. E.; Marcone, M.; Narine, S. S. On the structure of particulate gels. The case of salt-induced cold gelation of heat-denatured whey protein isolate. *Food Hydrocolloids* **2000**, *14*, 61−74.

(27) San Bagio, P. L.; Bulone, D.; Emanuele, A.; Palma, M. U. Self-assembly of biopolymeric structures below the treshold of random cross-link percolation. *Biophys. J.* **1996**, *70*, 494−499.

(28) Tobitani, A.; Ross-Murphy, S. B. Heat-induced gelation of globular proteins. 1. Model for the effects of time and temperature on the gelation time of BSA gels. *Macromolecules* **1997**, *30*, 4845−4854.

(29) Renard, D.; Rober, P.; Garnier, C.; Dufour, E.; Lefebvre, J. Gelation by phase separation in a whey protein system: in-stu kinetics of aggregation. *J. Biotechnol*. **2000**, *79*, 231−244.

(30) Aymard, P.; Durand, T.; Nicolai, T.; Gimel, J. C. Fractality of globular protein aggregates: from the molecular to the microscopic level. *Fractals-An Interdisciplinary Journal on the complex Geometry of Nature*. **1997**, *5*, 23−43.

(31) Le Bon, C.; Nicolai, T.; Durand, D. Growth and structure of aggregates of heat-denatured b-lactoglobulin. *Int. J. Food Sci. Technol*. **1999**, *34*, 451−465.

Received for review September 4, 2002. Revised manuscript received February 6, 2003. Accepted March 6, 2003.

JF0209342